Real-world application benchmark for QAOA algorithm for an electromobility use case

Marika Federer[1], Daniel Müssig [2], Steve Lenk[3], Jörg Lässig[4]

Abstract: To reduce CO_2 emissions in the mobility sector, battery electric service vehicles might play an important role in the future. Here, an optimal charging scheduling use case will be presented which includes local solar power generation for minimizing the power grid usage for electric service vehicles. Different formulations of the use case are given to illustrate the differences for classical and quantum-based optimization using a mixed integer linear program and a quadratic unconstrained binary optimization program, respectively. Addtionally, we study the complexity of our benchmark experiments by characterizing the respective QUBO matrices and the optimization landscapes. It is shown how the setting of the parameters of a certain experiment and its penalty function influences the complexity for a quantum-based optimizer. Additionally, we present a comparison of the computing times and summarize the current state of gate-based quantum computing for electromobility.

Keywords: QAOA; Electromobility; Quantum Computing; Energy

1 Introduction

Reducing greenhouse gases dramatically is one of the major challenges in the near-term future. To achieve this goal within the mobility sector, by assuming that the number of electric vehicles worldwide registered will rise to 140 million or more by 2030 [ABG+20], it is obvious that the mobility sector might have a large impact in that challenge. However, optimal utility of fluctuating renewable energy generation is a requirement to achieve CO_2-neutral charging of electric vehicles. Next to the private sector, the service sector has to reduce its emissions, here we investigate the optimization of a charging scheduling problem for electric service vehicles of an airport. Based on the proposed progress of quantum computing for optimization applications, we present an approach which can be used for gate-based quantum computing and quantum annealing.

2 Model formalism and benchmark

We consider a system at the airport Erfurt-Weimar to charge a couple of electric service vehicles based on the flight schedule and the availability of photovoltaic (PV) electricity

[1] Fraunhofer IOSB-AST, Dep. Cognitive Energy Systems, Ilmenau, Germany marika.federer@iosb-ast.fraunhofer.de
[2] Fraunhofer IOSB-AST, Dep. Cognitive Energy Systems, Görlitz, Germany daniel.muessig@iosb-ast.fraunhofer.de
[3] Fraunhofer IOSB-AST, Dep. Cognitive Energy Systems, Ilmenau, Germany steve.lenk@iosb-ast.fraunhofer.de
[4] University of Applied Sciences Zittau/Görlitz, Brückenstraße 1, 02826 Görlitz, Germany jlaessig@hszg.de

doi:10.18420/inf2022_97

generation.
The target is to optimize the charging schedule for several service electric vehicles (EVs) in accordance with the flight schedule by using predominantly the electricity generated by a roof-top photovoltaic station to minimize the electricity costs and the CO_2 emissions.
The classical optimization problem can be formulated using unit-less values as an integer linear problem

$$z = min \left(\sum_t |j(t) - pv(t)| \right) \tag{1}$$

$$\text{w. r. t.} \quad j(t) \leq j_{max}(t) \tag{2}$$

$$\sum_t j(t) \geq e_{min} \tag{3}$$

$$\sum_t j(t) \leq e_{max} \, . \tag{4}$$

with the PV power forecast time series $pv(t)$, the (aggregated) maximal charging power forecast $j_{max}(t)$, the minimal and maximal charging energies e_{min} and e_{max}. Eq. (1) is our target (or cost) function of the integer linear program.
However, for the use of quantum computing, i. e., quantum annealing and quantum approximate optimization algorithm (QAOA) for gate-based quantum computing, the optimization problem is usually written as a quadratic unconstrained binary optimization (QUBO) problem [Ko14; Lu14]. Therefore, we replace the absolute value function of the target function by a square function. This step causes that certain entangled states of the original expression might be shifted to higher target values. However, these states contain higher charging power peaks, which might negatively affect the electric grid and, thus, should be generally avoided, i. e., this shift does not alter our optimization problem negatively.
The constraints have to be included into the target function, which can be done using quadratic penalty functions and penalty factors.
To yield the QUBO representation, the integer values $j(t)$ are mapped to an appropriate binary representation [Kü21; Lu14]

$$j(t) = \sum_{n=0}^{b(t)-2} 2^n j_n + (j_{max}(t) - 2^{b(t)-1} + 1) \, j_{b(t)-1} \, . \tag{5}$$

with the necessary number of binary variables $b(t) := \lceil \log_2(j_{max}(t) + 1) \rceil$. This choice of binary representation already ensures the first constraint (2) and, thus, only two penalty functions have to be considered.
The QUBO formulation of the optimization model representing the target function in eq. (1) as well as the two constraints of eqs. (3)-(4) can be written as

$$z = min \left(\sum_t (j(t) - pv(t))^2 + C_a + C_b \right) \tag{6}$$

where

$$C_a = P_a \left(\sum_t j(t) - t - e_{min} \right)^2 \tag{7}$$

$$C_b = P_b \left(\sum_t j(t) + v - e_{max} \right)^2 . \tag{8}$$

To obtain the quantum mechanical Hamiltonian [Lu14], the binaries are substituted in eq. (5) by

$$j_n = \frac{1}{2} \left(1 + \sigma_n^z \right) , \tag{9}$$

to act on respective qubits.
To be able to compare classical solvers and the hybrid quantum classical algorithm QAOA [FGG14], we created a benchmark consisting of 28 experiments with different complexity and varying number of binaries/qubits ranging from 3 to 23. The amount of qubits is limited by the quantum hardware. As an example, the experiment 28 of our benchmark is visualized in Fig. 1. The parameters can be found in Tab. 1

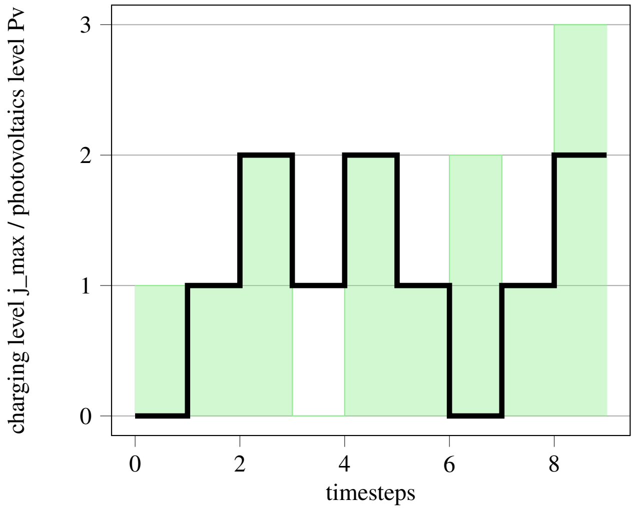

Fig. 1: Visualization of the input time series for experiment 28. The PV forecast time series $pv(t)$ is given in green, whereas the maximal charging power forecast $j_{max}(t)$ is marked by the bold black line.

3 Complexity

The details for four specific benchmark experiments are given in Tab. 1 to represent our complexity study. It can be seen from table that the number of time steps is increased

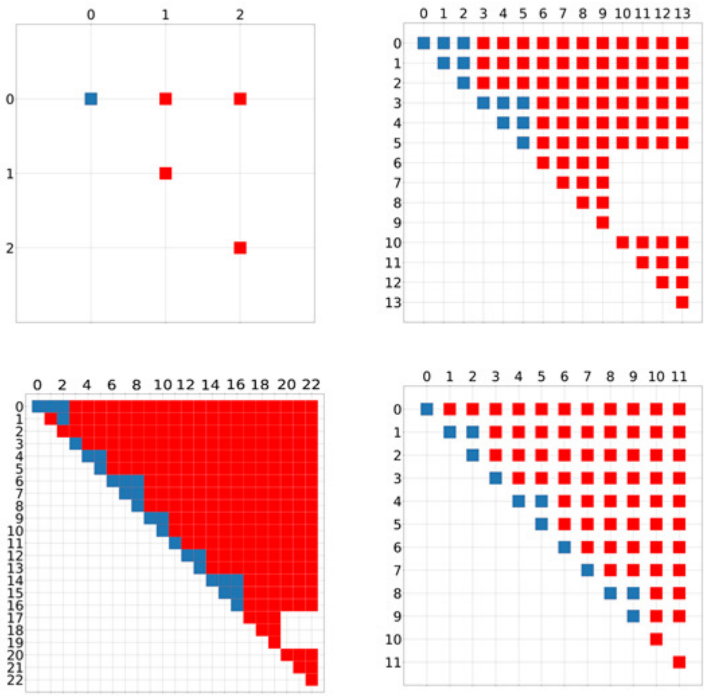

Fig. 2: Overview of QUBO matrices for experiments 1 (upper left), 7 (upper right), 27 (lower left) and 28 (lower right).

Tab. 1: Details of selected benchmark experiments

exp.	$\vec{j}_{max}$	$\vec{pv}$	e_{min}	e_{max}	nr. qubits
1	$[0,1]$	$[0,1]$	0	1	3
7	$[7,5]$	$[10,3]$	1	10	14
27	$[5,1,2,4,2,1,3,4]$	$[1,3,2,5,2,1,2,4]$	2	5	23
28	$[0,1,2,1,2,1,0,1,2]$	$[1,1,2,0,2,1,2,1,3]$	0	1	12

for the selected experiments 1 to 28. However, the number of qubits increases only from experiment 1 to 27 and it is reduced in experiment 28 compared to 27. This is due the reduction of the maximal number of charging levels j_{max} (from 5 in exp. 27 to 3 in exp. 28). Thus, the largest number of qubits is found for exp. 27 due to a combination of the number of time steps and charging levels.

To study the complexity of the combinatorial optimization program, we show the QUBO matrices of the selected experiments in Fig. 2. The non-zero qubits related to the optimization variable j representing the cost function are marked in blue, whereas the penalties causes the qubits marked in red to be non-zero. Obviously, the most of the non-zero elements in the QUBO matrix originates from the penalties since eqs. (7) and (8) describe global penalties, i. e., corresponds to interactions between all j qubits. Another remarking point is that there are qubits, which are not included in the cost function but represents the slack variables t and v in the penalty terms of eqs. (7) and (8). Their number is determined by the values of the binary representation of parameters e_{min} and e_{max}. Although the cost function includes rather limited coupling of the qubits, it is observable that an increase of the maximal charging levels $j_{max}(t)$ at a certain time step t yield to an interaction of the qubits representing the integer value j as a binary, see the blue marked elements in Fig. 2, e. g., for exp. 7. Since for future applications, a large amount of charging levels is expected, this increase in complexity should be considered for a strategy to achieve quantum advantage with shallow circuits [BGK18] in this special application case.
Since the coupling of the QUBO matrix does not necessarily correspond to a increase in complexity in the optimization landscape for the quantum approximate optimization algorithm [FGG14] with $p = 1$, we also study the landscape in Fig. 3. The optimization landscape corresponds to the expectation value of the sampled cost functions. In Fig. 3, we show the landscapes for experiments 1 (upper part) and 7 (lower part). On the left of fig. 3, the landscape is drawn for the program without penalties, i. e., $C_a = C_b = 0$, and on the right, it is shown considering the penalties. As indicated by the QUBO matrices, the penalties complicate the optimization landscape by increasing the number of local minima but also by increasing the variance of the landscape. Both effects might yield to problems for the classical optimizer of the QAOA algorithm to find the optimal values for the parameters γ and β for the cost Hamiltonian and the mixing Hamiltonian, respectively.

4 Summary and Outlook

We have shown the formulation of a real-world application using MILP and QUBO models and the involved complexity for the QUBO model using a visualization of its matrices and the optimization landscape. The next step will be to analyze if a measure of complexity can be found based on the optimization landscape and if it can be estimated using only the (easily available) QUBO matrix. Since the main part of the coupling terms within the QUBO matrices arises from the global penalties, different implementations of the penalties will be considered in future works. Here, a promising approach seems to be an implementation using conditional gates or a dynamic decoupling approach [De22].
Additionally, we will study if a QAOA algorithm can be used to solve benchmark experiments resembling real-world application scenarios. We will build the algorithm for real quantum hardware and consider different transpiling, mapping and dynamic decoupling strategies to find the most suitable approach for our benchmark. Additionally, we will investigate the

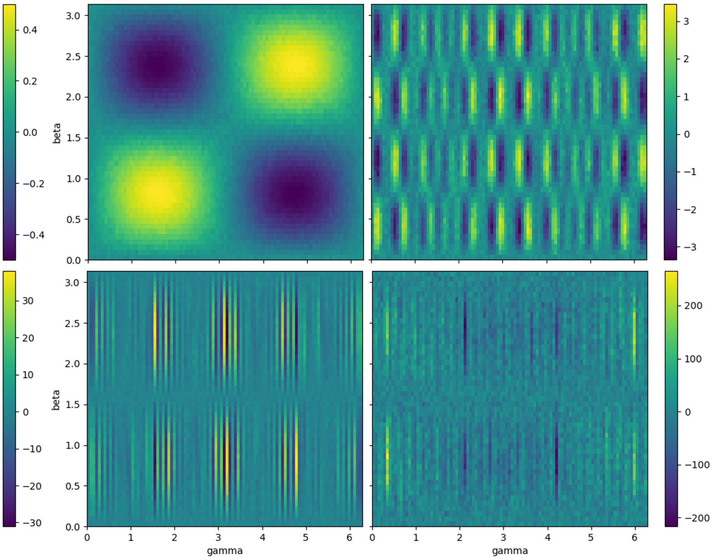

Fig. 3: Energy landscapes for experiments 1 (upper row) and 7 (lower row), without penalties (left column) and with penalties (right column).

influence of the classical and quantum part of the hybrid quantum-classical approach to discover bottlenecks and improvements.

Acknowledgment

This work was financially supported by the Bundesministerium für Wirtschaft und Energie through the project "EnerQuant" (Project- ID 03EI1025C). We thank Murad Babayev, Andreas Sturm, Fred Jendrzejewski, Yannick Deller, Sebastian Schmitt, Valentin Kasper and Philipp Hauke for fruitful and inspiring discussions.

References

[ABG+20] Abergel, T.; Bunsen, T.; Gorner, M., et al.: Global EV Outlook 2020 - Entering the decade of electric drive? 2020.

[BGK18] Bravyi, S.; Gosset, D.; König, R.: Quantum advantage with shallow circuits. Science 362/, pp. 308–311, 2018.

[De22] Deller, Y.; Schmitt, S.; Lewenstein, M.; Lenk, S.; Federer, M.; Jendrzejewski, F.; Hauke, P.; Kasper, V.: Quantum approximate optimization algorithm for qudit systems with long-range interactions, 2022, URL: https://arxiv.org/abs/2204.00340.

[FGG14] Farhi, E.; Goldstone, J.; Gutmann, S.: A Quantum Approximate Optimization Algorithm, https://arxiv.org/pdf/1411.4028.pdf, 2014.

[Ko14] Kochenberger, G.; Hao, J.-K.; Glover, F.; Lewis, M.; Lü, Z.; Wang, H.; Wang, Y.: The unconstrained binary quadratic programming problem: a survey. J. Comb. Optim. 28/, p. 58, 2014.

[Kü21] Küstner, M.: Modellierung von Problemen als quadratische unrestingierte binäre Optimierungsprobleme, Bachelor Thesis, TU Ilmenau, Department of Mathematics and Natural Sciences, 2021.

[Lu14] Lucas, A.: Ising formulations of many NP problems. Frontiers in Physics 2/5, https://www.frontiersin.org/article/10.3389/fphy.2014.00005, p. 1, 2014.